ACS Macro Letters

Letter

pubs.acs.org/macroletters

Positively Charged Dendron Micelles Display Negligible Cellular Interactions

Ryan M. Pearson,[†] Niladri Patra,[§] Hao-jui Hsu,[†] Sayam Uddin,[†] Petr Král,[§,∥] and Seungpyo Hong*[,†,‡]

[†]Departments of Biopharmaceutical Sciences, [‡]Bioengineering, [§]Chemistry, and [∥]Physics, University of Illinois at Chicago, Chicago, Illinois 60612, United States

Supporting Information

ABSTRACT: PEGylated dendron-based copolymers (PDCs) with different end-group functionalities (−NH_2, −COOH, and −Ac) were synthesized and self-assembled into dendron micelles to investigate the effect of terminal surface charges on size, morphology, and cellular interactions of the micelles. All of the dendron micelles exhibited similar sizes (20−60 nm) and spherical morphologies, as measured using dynamic light scattering and transmission electron microscopy, respectively. The cellular interactions of dendron micelles were evaluated using confocal microscopy and flow cytometry. Surprisingly, although amine-terminated dendrimers are known to strongly interact with cells nonspecifically, all of the surface-modified dendron micelles exhibited charge-independent low levels of cellular interactions. The unexpected results, particularly from the amine-terminated dendron micelles, could be attributed to: (i) minimal end-group effects, as each PDC has an approximately 10-fold lower charge-number-to-molecular-weight ratio compared to the dendrimer, and (ii) intra- and intermolecular hydrogen bonding between positively charged terminal groups with poly(ethylene glycol) (PEG) backbones, which leads to the sequestration of the charges, as demonstrated by atomistic molecular dynamics simulations. With the narrow size distribution, uniform morphologies, and low levels of nonspecific cellular interactions, the dendron micelles offer a promising drug delivery platform.

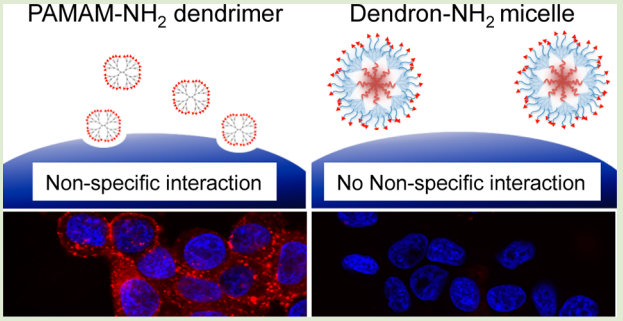

Designing a nanocarrier that elicits controlled biological properties is critical to develop highly effective multifunctional drug delivery platforms. It has been demonstrated that the cellular interactions of such nanocarriers can be modulated through control over size, morphology, hydrophobicity, and surface charge.[1] Among the numerously investigated nanomaterials, dendrimers are unique macromolecules that have been successfully developed as a drug delivery platform. Their well-defined molecular architecture coupled with advantageous properties such as high branching degree, flexibility, controllable surface chemistry, and multivalency have all been implemented, in one way or another, to enhance the efficacy of modern drug delivery platforms.[2]

Modulation of the surface charge of dendrimers has been used as major design criteria to control their cellular interactions and toxicity.[3] In general, positively charged amine-terminated (−NH_2) dendrimers display a high level of nonspecific cellular interactions and toxicity because of electrostatic interactions with negatively charged cell membranes, whereas negative and neutral-charged dendrimers (carboxylated (−COOH) or acetylated (−Ac) surfaces) do not.[3b,f,g] A number of other polycationic polymers, such as poly(L-lysine) (PLL), polyethylenimine (PEI), and diethylaminoethyl (DEAE)-dextran, have also shown nonspecific, spontaneous cellular interactions, which leads to high toxicity.[3h]

Recently, we have developed methoxy-terminated (−OMe) PEGylated dendron-based copolymers (PDC-OMe), which are triblock copolymers comprised of a polyester dendron (Generation 3 (G3), eight surface groups) and two types of linear polymers (polycaprolactone (PCL) and poly(ethylene glycol) (PEG)) (see Scheme 1 for the chemical structure).[4] At similar hydrophilic−lipophilic balances (HLBs), PDCs self-assembled into dendron micelles with high thermodynamic stability as measured by critical micelle concentrations (CMCs) that were 1−2 orders of magnitude lower than those of linear-block copolymer (LBC) counterparts. Additionally, molecular dynamics (MD) simulations revealed that the surface of the dendron-OMe micelle was almost completely covered by a dense PEG outer layer as opposed to the LBC micelles, which is expected to be beneficial by imparting "stealth" properties to the micelles in vivo.[5]

To understand the cellular interactions of dendron micelles at the molecular level, we engineered the chemical structure of each PDC to be suitable for self-assembly and to display various end-group functionalities on their surface. To that aim, we hypothesized that the surface functionality of the formed

Received: October 10, 2012
Accepted: December 26, 2012
Published: December 31, 2012

Scheme 1. Synthesis of Surface-Modified PDCs from PCL-G3-PEG-NH_2 (PDC-NH_2), PCL-G3-PEG-COOH (PDC-COOH), PCL-G3-PEG-Ac (PDC-Ac), and PCL-G3-PEG-RHO-Ac (PDC-RHO)

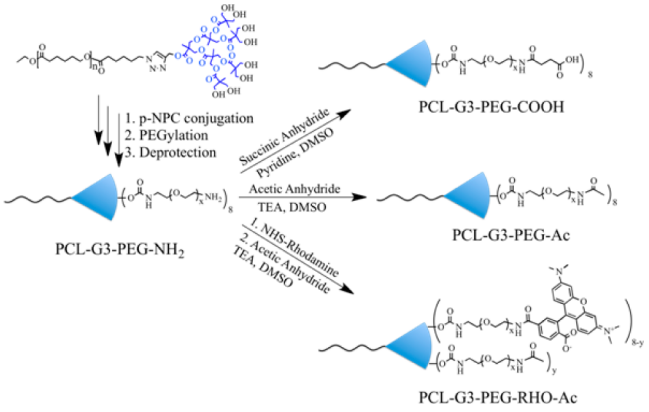

dendron micelles would largely determine these interactions, as in dendrimers and other nanocarriers. It was expected that amine-terminated dendron micelles would tend to interact spontaneously with cell membranes, while negative and neutral-charged micelles would exhibit low levels of cellular interactions. To test this hypothesis, four structurally similar PDCs that varied only by surface functional group (−NH_2, −COOH, −Ac, and −OMe) were synthesized and self-assembled into dendron micelles. The cellular interaction of each micelle was evaluated using confocal microscopy and flow cytometry. Surprisingly, we observed that all four dendron micelles displayed similar cellular uptake and cell-associated fluorescence. This finding disproved our hypothesis and prompted a thorough investigation of the potential reasons for these observations, such as size, morphology, surface charge density, and end-group orientation of the dendron micelles.

The synthesis of PDC-NH_2, PDC-COOH, and PDC-Ac with low polydispersity indices (PDI < 1.2) was completed using a modified pre-existing protocol (Scheme 1 and Table 1).[4] The

Table 1. Molecular Weight and Polydispersity Indices (PDIs) of Synthesized PDCs

samples	theoretical M_w	M_n[a]	$M_{n,GPC}$[b]	PDI
PDC-BOC	20 482	21 330	15 684	1.19
PDC-NH_2	19 690	18 077	-	N/A[c]
PDC-COOH	20 042	17 831	13 960	1.17
PDC-Ac	20 026	18 453	14 687	1.18
PDC-OMe[4]	21 990	22 568	15 690	1.02

[a]Number-averaged molecular weight, M_n, estimated by ^{1}H NMR. Measured by GPC using the following. [b]Conventional calibration against polystyrene standards. [c]Eluted as multiple broad peaks due to column interaction.[6]

molecular weights of the hydrophobic PCL tail and the hydrophilic PEG chains were 3.5 and 2 kDa, respectively. Each surface-modified PDC was synthesized through a series of steps starting from BOC-protected PDC (PDC-BOC). Deprotection of PDC-BOC resulted in amine-terminated PDC (PDC-NH_2), and subsequent carboxylation using succinic anhydride or acetylation using acetic anhydride resulted in PDC-COOH and PDC-Ac, respectively. Details of the synthesis and characterization (^{1}H NMR) of each PDC can be found in the Supporting Information (Figures S1−S3 of the Supporting Information). The dendron micelles with various surface groups were prepared by the self-assembly of the individual PDCs using the dialysis method and immediately used for further experiments (see details in the Supporting Information).

Figure 1A,B shows the particle size distribution, zeta potential, and CMC for dendron micelles of the four different

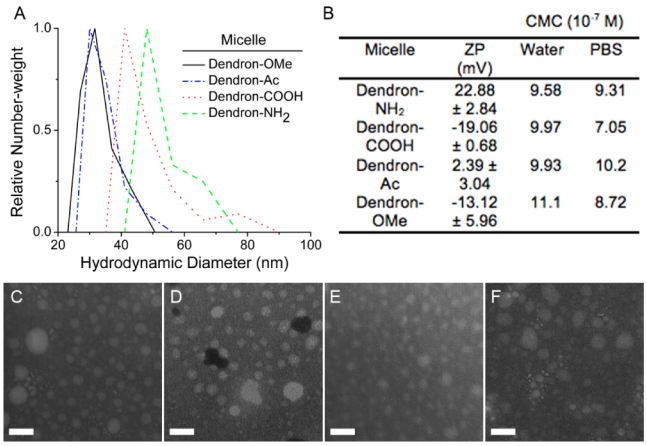

Figure 1. Characterization of surface-modified dendron micelles. (A) Hydrodynamic diameter measurements of dendron micelles using dynamic light scattering. (B) Zeta potential (ZP) values measured in ddH_2O (pH 5.6) and critical micelle concentration (CMC) of dendron micelles measured in ddH_2O and PBS (pH 7.4). Transmission electron micrographs of dendron micelles comprised of (C) PDC-NH_2, (D) PDC-COOH, (E) PDC-Ac, and (F) PDC-OMe. Scale bar: 50 nm.

types. The micelles predominantly exhibited diameters of 20−60 nm, obtained by dynamic light scattering (DLS). Their particle sizes were stable for up to 21 days at room temperature in water (data not shown) and had the zeta potentials between −20 and 23 mV. The negative zeta potential value of the dendron-OMe micelles is likely attributed to the presence of partially negatively charged oxygen atoms near the termini of the PEG chain and is in agreement with a previous report employing methoxy-terminated polymer micelles.[7] The zeta potential of the dendron-Ac micelles was close to neutral because the proton in the amide end group does not appreciably dissociate at pH 5.6 (ddH_2O) due to its high pK_a value (typically >15), maintaining a neutral zeta potential.

The thermodynamic stability of the PDCs was evaluated by measuring the CMC through monitoring their micelle formation with pyrene used as a fluorescent probe in water and in PBS (Figure S4 of the Supporting Information).[8] As expected, the surface-modified PDCs displayed very low CMCs on the order of 10^{-7} M at high hydrophilic−lipophilic balances (HLB) of ∼16.5. HLB is defined as $20 \times M_H/(M_H + M_L)$, where M_H is the mass of the hydrophilic portion and M_L is the mass of the lipophilic portion of an amphiphilic molecule.[4,9] The CMCs of the PDCs measured in water and PBS appeared to be very similar under the conditions tested. For cell-level experiments based on fluorescence detection, a rhodamine-labeled PDC (PDC-RHO) was synthesized from PDC-NH_2 and incorporated at 10 wt % into each micelle through mixing of PDCs before micelle formation (Scheme 1 and the Supporting Information).

Next, we investigated cellular interactions of the dendron micelles. KB cells were treated with the dendron micelles at a

dx.doi.org/10.1021/mz300533w | ACS Macro Lett. 2013, 2, 77−81

polymer concentration of 4 μM (>4-fold over CMC) to ensure that the structure of each micelle remained intact. Rhodamine-labeled, amine-terminated G4 polyamidoamine (PAMAM) dendrimer was prepared as described in our previous studies[3i,10] and was used as a positive control in the cell studies at a concentration of 1 μM (Figure 2A). Differences in

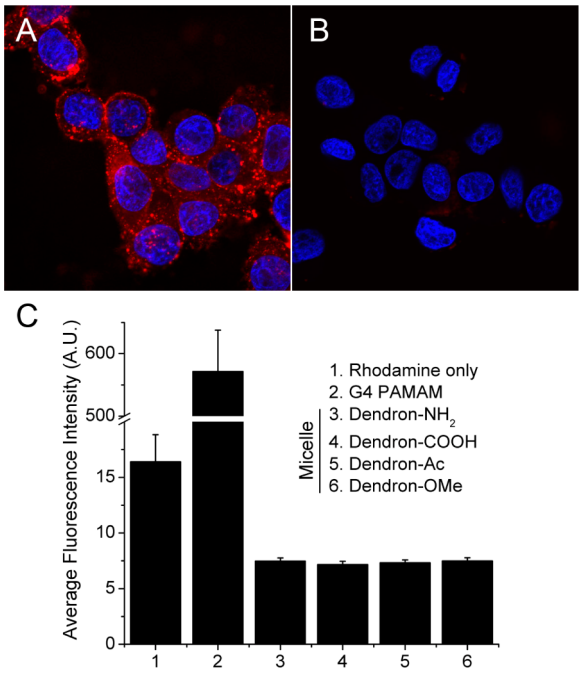

Figure 2. Cellular uptake and association of rhodamine-labeled G4 PAMAM dendrimers and surface-modified dendron micelles. KB cells were treated with (A) G4 PAMAM dendrimer and (B) dendron-NH_2 micelles. Note that dendron micelles, regardless of their surface charges, do not exhibit nonspecific cellular interactions unlike positively charged dendrimers. (C) Flow cytometry results of the cellular association of G4 PAMAM and dendron micelles. Experiments were carried out for 60 min. Nuclei were stained using DAPI (blue color).

the concentration of polymers used in the cell experiments are due to the normalization of rhodamine content between samples (dendrimer has a higher rhodamine amount than dendron micelles by 4-fold). This normalization allowed for the direct comparison of levels of cellular interaction using confocal microscopy and flow cytometry.

Unexpectedly, the dendron-NH_2 micelles did not exhibit a higher cellular uptake or cell-associated fluorescence than other surface-modified micelles (Figure 2B and C and Figure S5 of the Supporting Information). Instead, all surface-modified dendron micelles showed similar cellular uptake and low cell-associated fluorescence. The results from the dendron-NH_2 micelle are in contrast to our positive control achieved with PAMAM-NH_2 dendrimers, where we found that after 60 min of incubation a significant amount of the dendrimers was interacting with the cells (Figure 2A and C). Our observations related to the dendron-NH_2 micelles are also in contrast with the results of previous reports, where the cellular interactions of G5 and G7 PAMAM dendrimers with $-NH_2$, $-COOH$, and $-Ac$ end-group modifications were tested.[3b,f] PAMAM-NH_2 dendrimers strongly interacted with KB cells, while PAMAM-COOH and PAMAM-Ac dendrimers did not exhibit any significant cellular interactions after the same 60 min incubation time. In addition to studies using other dendrimers,[3d,11] negatively charged PEGylated gold nanoparticles (GNPs) have shown limited cellular uptake, and yet positively charged PEGylated GNPs showed significant cellular uptake.[12] Liposomes prepared from positive, negative, neutral, and neutral-PEG lipids have been also evaluated for their cellular uptake behaviors. It was found that the liposomes interact with cells in a charge-dependent manner, where the degree of nonspecific cellular interaction goes with the charge as: positive > neutral > negative.[13]

To understand this unexpected behavior of the dendron micelles, we investigated a number of parameters, such as size, morphology, PEG density, and orientation of the end groups, which may play roles in determining the cellular interactions of the dendron micelles. Note that nanocarrier−cell interactions are complex and potentially affected by a number of factors.[1e] We used transmission electron microscopy (TEM) to evaluate the effect of size and morphology of the dendron micelles. Figure 1C−F shows electron micrographs of the dendron micelles after negative staining with 2% phosphotungstic acid. The size of the dendron micelles observed using TEM correlated with the results obtained using DLS. The micelles also had a spherical morphology, confirming our previous results (Figure 1).[4]

One possible reason for the absence of observable cellular interactions for the four types of dendron micelles could be their unusually dense PEG layer due to the dendritic architecture, as demonstrated in our previous study.[4] PEG is well-known to enhance the evasion of nanoparticles from detection by the reticuloendothelial system (RES) in vivo.[14] However, the presence of PEG does not always prevent micelles from nonspecifically interacting with cells.[15] For amphiphilic polymers that comprise micelles with relatively low HLBs (typically lower than 3), a significant degree of nonspecific interactions with cell surfaces has been observed as opposed to those from higher HLB polymers (higher than 8 in general).[16]

In our dendron micelles, a PDC molecule theoretically accommodates eight PEG arms, resulting in an extraordinarily high PEG density on the PDC surface. Atomistic MD simulations revealed that the PEG density is significantly increased when the number of PEG chains per PDC is increased (Figure S6 of the Supporting Information). This high PEG density, along with the almost complete surface coverage of the PEG outer layer,[4] could likely result in the maximized nonfouling effect of PEG, which would, in turn, minimize nonspecific interactions of the dendron micelles in vitro regardless of the surface charge.

Another reason for the weak cellular interactions of the dendron micelles could be their significantly higher ratio of molecular weight to surface functional groups. Each PDC has an approximate molecular weight of 18 000 Da and eight end groups, resulting in a high molecular-weight-to-surface-functional-group ratio (~2250). G4 PAMAM dendrimers with an ethylenediamine core on the other hand have a theoretical molecular weight of 14 215 Da and 64 end groups, resulting in a 10-fold lower ratio (~222). One can thus expect that the end-group effect of the dendron micelles should be smaller than in dendrimers.

We also investigated the effect of end-group orientation, which may contribute to the unobservable cellular interactions of the dendron-NH_2 micelles. The hydrogens of the amino-functional groups on the micelle surface could interact through

dx.doi.org/10.1021/mz300533w | ACS Macro Lett. 2013, 2, 77−81

hydrogen bonding with the oxygen atoms of the PEG backbone, in analogy to the coupling observed from other ions.[17] This would result in a decreased number of available positive charges to interact with the plasma membrane. This charge sequestration may be one potential mechanism by which the dendron-NH_2 micelles exhibit limited cellular interactions.

To confirm the intramolecular hydrogen bond formation and compare the overall micelle parameters, we performed atomistic MD simulations. Since our aim was to investigate the orientation of each of the employed end groups, it was not necessary to match the size of the experimentally produced micelles. Dendron micelles were simulated using 30 PDCs arranged into spherical micelles (Figure S7 of the Supporting Information). The simulated dendron micelle data are presented in Table S1 of the Supporting Information. The PCL core size of each micelle was similar (~8 nm), and the average thickness of the surface-modified PEG layers ranged between 10 and 11 nm. To observe the details of intramolecular hydrogen bond formation, three different simulations were carried out, each of them containing a single PEG chain that was terminated by one of the functional groups, $-NH_3^+$, −Ac, or $-COO^-$ (see details in the Supporting Information). Hydrogen bonding between amine-hydrogens and oxygen atoms of the PEG chains was evaluated using a cutoff distance of 2.75 Å. From these simulations, we found that the PEG chain wraps around the terminal amine group through hydrogen bonding, as seen in Figure 3. No hydrogen bonding was observed between PEG and the other end groups used in this study. Although we focused on one PEG chain in this simulation due to the long equilibrium time required, in principle, the hydrogen bond formation should be present throughout the whole micelle, both intra- and intermolecularly. This phenomenon is likely responsible for the decreased presentation of positive charges at the surface of the dendron-NH_2 micelles, contributing to the reduced cellular interactions.

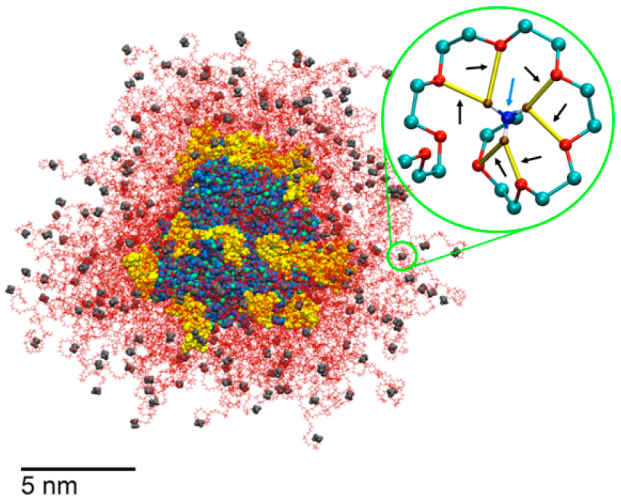

Figure 3. Atomistic molecular dynamics simulations of the dendron-NH_3^+ micelle in water. Black arrows indicate hydrogen bonding (yellow bonds) between hydrogens (gold balls) present on the terminal amine group (blue ball; identified by a blue arrow) with the oxygen atoms (red balls) present on the PEG chain. The hydrogen bond cutoff distance is 2.75 Å. We expect to observe intra- as well as intermolecular hydrogen bond formation within the micelle. Water is not shown for clarity.

To further identify differences between PDCs and dendrimers, cytotoxicity experiments were performed using PDCs and G4 PAMAM dendrimers at concentrations from 0.1 to 100 μM. PDCs did not display any significant toxicity to KB cells, whereas dendrimers were toxic at concentrations above 1 μM, as measured using MTS assay after 24 h incubation (Figure S8 of the Supporting Information). This result was expected for neutral and negative-charged PDCs; however, the difference in toxicity between PDC-NH_2 and PAMAM dendrimers[3f] further confirms that the effect of end groups on determining cytotoxicity, as observed for dendrimers, is most likely negligible for our dendron micelles.

In summary, we have presented the synthesis of three new types of surface-modified PDCs, with $-NH_2$, −COOH, −Ac, and −OMe surface groups and systematically studied their interactions with cells. These micelles did not exhibit charge-dependent cellular interactions, as hypothesized based on the previous observations from PAMAM dendrimers. The lack of cellular interaction for the dendron-NH_2 micelles could be attributed to the dense PEG layers, the high molecular-weight-to-surface-group ratio (~2250), and the orientation of end groups (charge sequestration via hydrogen bond formation). Our results show that surface modification of the dendronized copolymers does not significantly alter the size or morphology of the formed micelles. Additionally, we have demonstrated that the dendron micelles are nontoxic up to concentrations of 100 μM, which is highly beneficial for PDCs to be accepted as a potential drug delivery platform. These results provide a guideline for designing highly effective and targeted drug delivery micelles by overcoming, at times, the nonspecific interactions associated with PEGylated nanocarriers.

■ ASSOCIATED CONTENT

Supporting Information

Detailed experimental and computational protocols, ^1H NMR spectra, CMC plots, additional cell uptake images, additional simulation figures, and MTS assay results. This material is available free of charge via the Internet at http://pubs.acs.org.

■ AUTHOR INFORMATION

Corresponding Author

*E-mail: sphong@uic.edu.

Notes

The authors declare no competing financial interest.

■ ACKNOWLEDGMENTS

This work was supported by the Hans W. Vahlteich Research Fund awarded to S.H. from the University of Illinois Foundation and was conducted in a facility constructed with support from the NIH (grant# C06RR15482). R.M.P. acknowledges the partial support from a Predoctoral Fellowship in the Pharmaceutical Sciences from the American Foundation for Pharmaceutical Education (AFPE). N.P. acknowledges the support from the UIC Harbert E. Paaren Academic Year Research Fellowship. The calculations were performed on the NERSC supercomputer networks.

■ REFERENCES

(1) (a) Kataoka, K.; Harada, A.; Nagasaki, Y. *Adv. Drug Delivery Rev.* **2001**, *47*, 113−131. (b) Duncan, R. *Nat. Rev. Drug Discovery* **2003**, *2*, 347−60. (c) Peer, D.; Karp, J. M.; Hong, S.; Farokhzad, O. C.; Margalit, R.; Langer, R. *Nat. Nanotechnol.* **2007**, *2*, 751−60. (d) Jin, S.-E.; Bae, J. W.; Hong, S. *Microsc. Res. Tech.* **2010**, *73*, 813−823.

(e) Zhao, F.; Zhao, Y.; Liu, Y.; Chang, X.; Chen, C.; Zhao, Y. *Small* **2011**, *7*, 1322−1337.
(2) (a) Hong, S.; Leroueil, P. R.; Majoros, I. n. J.; Orr, B. G.; Baker, J. R.; Banaszak Holl, M. M. *Chem. Biol.* **2007**, *14*, 107−115. (b) Lee, C. C.; MacKay, J. A.; Frechet, J. M. J.; Szoka, F. C. *Nat. Biotechnol.* **2005**, *23*, 1517−1526. (c) Myung, J. H.; Gajjar, K. A.; Saric, J.; Eddington, D. T.; Hong, S. *Angew. Chem., Int. Ed.* **2011**, *50*, 11769−11772. (d) Pearson, R. M.; Sunoqrot, S.; Hsu, H.-j.; Bae, J. W.; Hong, S. *Ther. Delivery* **2012**, *3*, 941−959.
(3) (a) Duncan, R.; Izzo, L. *Adv. Drug Delivery Rev.* **2005**, *57*, 2215−2237. (b) Hong, S.; Rattan, R.; Majoros, I. J.; Mullen, D. G.; Peters, J. L.; Shi, X.; Bielinska, A. U.; Blanco, L.; Orr, B. G.; Baker, J. R., Jr.; Holl, M. M. *Bioconjugate Chem.* **2009**, *20*, 1503−13. (c) Kitchens, K. M.; Kolhatkar, I. B.; Swaan, P. W.; Ghandehari, H. *Mol. Pharmaceutics* **2008**, *5*, 364−369. (d) Perumal, O. P.; Inapagolla, R.; Kannan, S.; Kannan, R. M. *Biomaterials* **2008**, *29*, 3469−3476. (e) Albertazzi, L.; Serresi, M.; Albanese, A.; Beltram, F. *Mol. Pharmaceutics* **2010**, *7*, 680−688. (f) Hong, S. P.; Bielinska, A. U.; Mecke, A.; Keszler, B.; Beals, J. L.; Shi, X. Y.; Balogh, L.; Orr, B. G.; Baker, J. R.; Holl, M. M. B. *Bioconjugate Chem.* **2004**, *15*, 774−782. (g) Leroueil, P. R.; Hong, S.; Mecke, A.; Baker, J. R.; Orr, B. G.; Banaszak Holl, M. M. *Acc. Chem. Res.* **2007**, *40*, 335−342. (h) Hong, S.; Hessler, J. A.; Banaszak Holl, M. M.; Leroueil, P.; Mecke, A.; Orr, B. G. *J. Chem. Health Saf.* **2006**, *13*, 16−20. (i) Yang, Y.; Sunoqrot, S.; Stowell, C.; Ji, J.; Lee, C.-W.; Kim, J. W.; Khan, S. A.; Hong, S. *Biomacromolecules* **2012**, *13*, 2154−2162.
(4) Bae, J. W.; Pearson, R. M.; Patra, N.; Sunoqrot, S.; Vukovic, L.; Kral, P.; Hong, S. *Chem. Commun.* **2011**, *47*, 10302−10304.
(5) (a) Owens, D. E., III; Peppas, N. A. *Int. J. Pharm.* **2006**, *307*, 93−102. (b) Ding, B. S.; Dziubla, T.; Shuvaev, V. V.; Muro, S.; Muzykantov, V. R. *Mol. Interventions* **2006**, *6*, 98−112.
(6) Yan, J.; Ye, Z.; Luo, H.; Chen, M.; Zhou, Y.; Tan, W.; Xiao, Y.; Zhang, Y.; Lang, M. *Polym. Chem.* **2011**, *2*, 1331−1340.
(7) Zhang, Y.; Zhang, Q.; Zha, L.; Yang, W.; Wang, C.; Jiang, X.; Fu, S. *Colloid Polym. Sci.* **2004**, *282*, 1323−1328.
(8) Gaucher, G.; Dufresne, M. H.; Sant, V. P.; Kang, N.; Maysinger, D.; Leroux, J. C. *J. Controlled Release* **2005**, *109*, 169−188.
(9) Becher, P.; Schick, M. J. *Nonionic Surfactants Physical Chemistry*; Marcel Dekker: New York, 1987; pp 435−491.
(10) Sunoqrot, S.; Bae, J. W.; Pearson, R. M.; Shyu, K.; Liu, Y.; Kim, D.-H.; Hong, S. *Biomacromolecules* **2012**, *13*, 1223−1230.
(11) (a) Kitchens, K. M.; Foraker, A. B.; Kolhatkar, R. B.; Swaan, P. W.; Ghandehari, H. *Pharm. Res.* **2007**, *24*, 2138−2145. (b) Kolhatkar, R. B.; Kitchens, K. M.; Swaan, P. W.; Ghandehari, H. *Bioconjugate Chem.* **2007**, *18*, 2054−2060. (c) Saovapakhiran, A.; D'Emanuele, A.; Attwood, D.; Penny, J. *Bioconjugate Chem.* **2009**, *20*, 693−701.
(12) Arnida; Malugin, A.; Ghandehari, H. *J. Appl. Toxicol.* **2010**, *30*, 212−217.
(13) Miller, C. R.; Bondurant, B.; McLean, S. D.; McGovern, K. A.; O'Brien, D. F. *Biochemistry* **1998**, *37*, 12875−12883.
(14) Veronese, F. M.; Pasut, G. *Drug Discovery Today* **2005**, *10*, 1451−1458.
(15) (a) Xiao, K.; Li, Y.; Luo, J.; Lee, J. S.; Xiao, W.; Gonik, A. M.; Agarwal, R. G.; Lam, K. S. *Biomaterials* **2011**, *32*, 3435−3446. (b) Hu, Y.; Xie, J.; Tong, Y. W.; Wang, C.-H. *J. Controlled Release* **2007**, *118*, 7−17.
(16) (a) Fan, W.; Wu, X.; Ding, B.; Gao, J.; Cai, Z.; Zhang, W.; Yin, D.; Wang, X.; Zhu, Q.; Liu, J.; Ding, X.; Gao, S. *Int. J. Nanomed.* **2012**, *7*, 1127−38. (b) Luxenhofer, R.; Sahay, G.; Schulz, A.; Alakhova, D.; Bronich, T. K.; Jordan, R.; Kabanov, A. V. *J. Controlled Release* **2011**, *153*, 73−82.
(17) Vukovic, L.; Khatib, F. A.; Drake, S. P.; Madriaga, A.; Brandenburg, K. S.; Kral, P.; Onyuksel, H. *J. Am. Chem. Soc.* **2011**, *133*, 13481−13488.